1
Introduction

Particle physics is the study of the properties of subatomic particles and of the interactions that occur among them. This book is concerned with the experimental aspects of the subject, including the characteristics of various detectors and considerations in the design of experiments. This introductory chapter begins with a description of the particles and interactions studied in particle physics. Next we briefly review some important material from relativistic kinematics and scattering theory that will be used later in the book. Then we give a brief preview of the various aspects of particle physics experiments, before discussing each topic in greater detail in subsequent chapters. Finally, we give a short discussion of some of the tasks involved in analyzing the data from an experiment.

1.1 Particle physics

Particle physics is the branch of science concerned with the ultimate constituents of matter and the fundamental interactions that occur among them. The subject is also known as high energy physics or elementary particle physics. Experiments over the last 40 years have revealed whole families of short-lived particles that can be created from the energy released in the high energy collisions of ordinary particles, such as electrons or protons. The classification of these particles and the detailed understanding of the manner in which their interactions leads to the observable world has been one of the major scientific achievements of the twentieth century.

The notion that matter is built up from a set of elementary constituents dates back at least 2000 years to the time of the Greek philosophers. The ideas received a more quantitative basis in the early nineteenth century with the molecular hypothesis and the development of chemistry. By the

Downloaded from https://www.cambridge.org/core. UNIVERSIDAD AUTONOMA METROPOLITANA, on 16 Nov 2026 at 19:59:29, subject to the Cambridge Core terms of use, available at https://www.cambridge.org/core/terms. https://doi.org/10.1017/9781009290098.002

end of the century most scientists accepted the idea that matter was constructed from aggregates of atoms. The discovery of radioactivity and the analysis of low energy scattering experiments in the early decades of this century revealed that atoms themselves had a structure. The experiments showed that the positive charge and most of the atomic mass was concentrated in a dense nucleus surrounded by a cloud of electrons.

The discipline of nuclear physics developed in the 1930s, particularly after the discovery of the neutron and the invention of particle accelerators. With sufficient energy the nucleus could be broken apart into its constituent protons and neutrons. At the same time physicists developed new particle detectors, such as Geiger tubes and cloud chambers, to study the properties of cosmic ray particles. The modern discipline of particle physics evolved in the late 1940s from a fusion of high energy nuclear physics and cosmic ray physics.

The chief concerns of this book are a description of the manner in which particles interact in matter, the properties of the detectors used to measure these interactions, and the fundamental considerations involved in designing a particle physics experiment. Two other very important aspects of the subject are data analysis and the interpretation of data using elementary particle theory. A brief survey of data analysis is given in the last section of this chapter. Fortunately, for particle theory an excellent introductory treatment is already available [1].

1.2 Particles and interactions

At the present, as best we can tell, four types of interactions are sufficient to explain all phenomena in physics. The interactions and their approximate relative strengths at distances $\sim 10^{-18}$ cm are [2]

1. strong nuclear, 1;
2. electromagnetic, 10^{-2};
3. weak nuclear, 10^{-5}; and
4. gravitational, 10^{-39}.

The gravitational force controls the interactions between massive bodies separated by large distances. However, the gravitational force between particles, where a typical mass is 10^{-27} kg, is so feeble that it does not appear to have a significant effect on elementary particle interactions. Thus, for particles the electromagnetic force dominates for distances down to 10^{-13} cm, where the nuclear forces begin to become important. The strong nuclear force is responsible for the binding of particles into nuclei, while the weak nuclear force is responsible for processes such as nuclear beta decay.

Downloaded from https://www.cambridge.org/core. UNIVERSIDAD AUTONOMA METROPOLITANA, on 16 Nov 2026 at 19:59:29, subject to the Cambridge Core terms of use, available at https://www.cambridge.org/core/terms. https://doi.org/10.1017/9781009290098.002

The electromagnetic interactions of particles can be calculated using the theory of quantum electrodynamics (QED). This is probably the most successful theory in all of physics and is capable of making extremely precise predictions. Recently a model has been developed that successfully treats the weak and electromagnetic interactions as the low energy manifestations of the breakdown of a unified electroweak interaction. A prediction of this model, which has recently been verified, is the existence of massive particles known as the $W^{\pm}$ and Z gauge bosons. Other grand unified models have been developed that assert that the electroweak and strong nuclear interactions have resulted from the breakdown of a single interaction. One consequence of these models is that the proton should have a small but finite probability of decaying.

Hundreds of new particles have been discovered in the study of high energy interactions. Many ways have been devised to group them into families with similar characteristics. One way to classify particles is by the type of interactions in which they participate. The leptons are particles that are not affected by the strong interaction. The electron, muon, and neutrino are examples of leptons. At present leptons appear to be truly elementary particles. They have no measured internal structure and are sometimes referred to as pointlike particles.

Particles that are affected by the strong interaction are known as hadrons. There are two main classes of hadrons. The baryons are hadrons with a half-integral value for the spin quantum number. The mesons, on the other hand, are hadrons with integral values of the spin quantum number. The pions are examples of mesons.

The lowest lying (least massive) baryons are the proton and the neutron. These two common constituents of nuclei are often referred to collectively as nucleons. The hyperons are unstable baryons that decay via the weak interaction and have a nonzero value for the internal quantum number known as strangeness. The lowest lying hyperon is the Λ particle. The decay chain of all unstable baryons ends with a final state containing a proton.

One of the early theories of the strong interaction, known as SU(3), predicted a relation among the baryon masses. Using this relation and the masses of the then-known baryons, it was possible to predict the existence of a hyperon with three units of strangeness, called the Ω^-. Figure 1.1 shows the historic bubble chamber photograph that proved the existence of the Ω^- hyperon. Its discovery marked an important milestone in our understanding of elementary particles.

The largest group of hadrons are referred to as resonances. These parti-

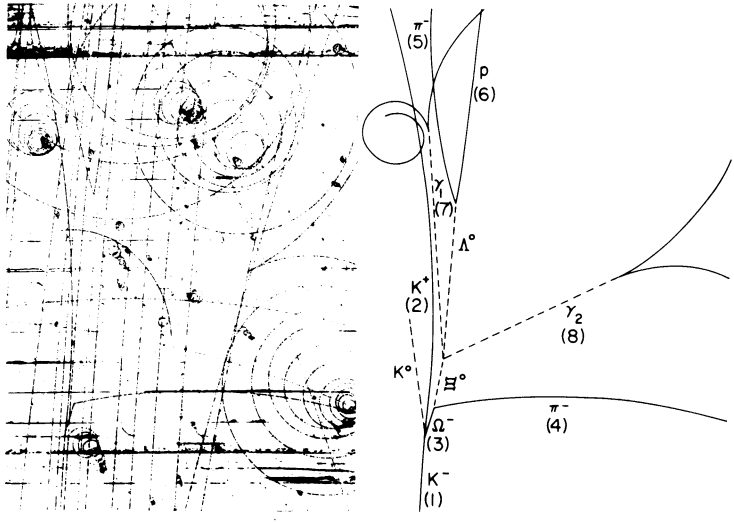
Downloaded from https://www.cambridge.org/core. UNIVERSIDAD AUTONOMA METROPOLITANA, on 16 Nov 2026 at 19:59:29, subject to the Cambridge Core terms of use, available at https://www.cambridge.org/core/terms. https://doi.org/10.1017/9781009290098.002

cles can decay via the strong interaction and thus have lifetimes on the order of 10^{-23} sec. Even traveling at the speed of light, this lifetime is much too short for the particles to travel a measurable distance in the lab. Thus, the properties of the resonances must be inferred from the properties of their longer-lived decay products.

Unlike the leptons, the hadrons are believed to have an internal structure. In the currently favored model of strong interactions (quantum chromodynamics, or QCD) hadrons are built up from pointlike spin $\frac{1}{2}$ objects known as quarks. The quarks are unlike other particles in several respects. The magnitude of their charge is one-third or two-thirds of the electron's charge, and free quarks have never been observed in scattering experiments. In the QCD model a quark attempting to leave the interior of a hadron would cause new quark–antiquark pairs to be created. The quarks and antiquarks would then recombine in such a way as to form new hadrons. Very energetic quarks would form a narrow spray of hadrons known as a jet.

Another remarkable feature of nature is the existence of antimatter. For every particle there is an antiparticle with the same mass and spin, but with opposite values for the charge and some of the internal quantum

Figure 1.1 The first bubble chamber photograph of the decay of an Ω^- hyperon. The picture was taken by a group headed by N. Samios at the 80-in. chamber at Brookhaven National Laboratory in 1964. (Courtesy of Brookhaven National Laboratory.)



Downloaded from https://www.cambridge.org/core. UNIVERSIDAD AUTONOMA METROPOLITANA, on 16 Nov 2026 at 19:59:29, subject to the Cambridge Core terms of use, available at https://www.cambridge.org/core/terms. https://doi.org/10.1017/9781009290098.002

numbers. A familiar example is the positron, which is the antiparticle of the electron.

Besides the leptons and the hadrons there is a third group of particles known as the gauge bosons. These integral spin particles are responsible for transmitting the basic interactions. The most well known example is the photon, which mediates the electromagnetic interaction. The weak interaction is thought to be mediated by the $W^{\pm}$ and Z vector bosons. According to QCD, the carriers of the strong interaction are massless particles known as gluons, while the gravitational interaction is thought to be mediated by spin 2 objects known as gravitons.

1.3 Relativistic kinematics

The mechanics of particle interactions must obey the laws of special relativity [3]. The velocity $\mathbf{v}$ of a particle is frequently specified in terms of the dimensionless quantity

$$\boldsymbol{\beta} = \mathbf{v}/c \tag{1.1}$$

where c is the speed of light in vacuum. The momentum and energy of the particle are given by

$$\mathbf{p} = mc\gamma\boldsymbol{\beta} \tag{1.2}$$

and

$$E = mc^2\gamma \tag{1.3}$$

where m is the mass of the particle measured in the reference frame in which it is at rest, and the auxiliary function γ is defined as

$$\gamma = (1 - \beta^2)^{-1/2} \tag{1.4}$$

The high energy behavior of various phenomena is frequently plotted as a function of γ. In these cases it may be convenient to rewrite the velocity and momentum in the form

$$\beta = [(\gamma^2 - 1)/\gamma^2]^{1/2} \tag{1.5}$$

and

$$p = mc(\gamma^2 - 1)^{1/2} \tag{1.6}$$

It is customary to measure energies in multiples of the electron volt (eV), typically MeV or GeV, at high energies. Then from Eq. 1.2 the unit of momentum is MeV/c, and from Eq. 1.3 the unit for mass is MeV/c^2. The constant c is frequently set to 1 to simplify relativistic calculations.

The energy and momentum of a particle in a second coordinate system moving with constant velocity $-\boldsymbol{\beta}_0$ with respect to the original (primed)

Downloaded from https://www.cambridge.org/core. UNIVERSIDAD AUTONOMA METROPOLITANA, on 16 Nov 2026 at 19:59:29, subject to the Cambridge Core terms of use, available at https://www.cambridge.org/core/terms. https://doi.org/10.1017/9781009290098.002

system is governed by the Lorentz transformation equations [3]

$$\begin{aligned} \mathbf{p} &= \mathbf{p}' + \boldsymbol{\beta}_0 \gamma \left(\frac{\gamma}{\gamma + 1} \boldsymbol{\beta}_0 \cdot \mathbf{p}' + \frac{E'}{c} \right) \\ \frac{E}{c} &= \gamma \left(\frac{E'}{c} + \boldsymbol{\beta}_0 \cdot \mathbf{p}' \right) \end{aligned} \tag{1.7}$$

For the special case when the transformation takes place along the z axis, the transformation equations simplify to

$$\begin{aligned} p_x &= p'_x \\ p_y &= p'_y \\ p_z &= \gamma \left(p'_z + \beta_0 \frac{E'}{c} \right) \\ \frac{E}{c} &= \gamma \left(\frac{E'}{c} + \beta_0 p'_z \right) \end{aligned} \tag{1.8}$$

The quantities $(E/c, \mathbf{p})$ can be interpreted as the components of a vector in a 4-dimensional space and are referred to as the energy–momentum 4-vector. The first quantity in the parentheses is denoted the 0th component.

Another important 4-vector is $(ct, \mathbf{x})$, where $\mathbf{x}$ is the position and t is time. The components of all 4-vectors obey transformation laws analogous to Eq. 1.8. An important consequence of the Lorentz transformation applied to this 4-vector is time dilation. Suppose that an interval of time τ elapses in a coordinate system where some particle is at rest. Time intervals in this frame are referred to as proper times. The corresponding time interval in a coordinate system moving with velocity $-\beta$ with respect to the particle (or equivalently in the frame where the particle has velocity $+\beta$) is

$$t = \gamma \tau \tag{1.9}$$

Thus, time intervals measured in a frame where the particle is moving are increased by the factor γ over the proper time intervals.

We shall identify 4-vectors by using a tilde, for example, $\tilde{a}$. The scalar product of two 4-vectors $\tilde{a}$ and $\tilde{b}$ is defined in the metric we are using as

$$\tilde{a} \cdot \tilde{b} = a_0 b_0 - \mathbf{a} \cdot \mathbf{b} \tag{1.10}$$

It follows immediately that the square of a 4-vector is

$$\tilde{a} \cdot \tilde{a} = a_0^2 - |\mathbf{a}|^2$$

As an example, consider the decay of an unstable particle into two particles with 4-momenta $\tilde{p}_1$ and $\tilde{p}_2$. The effective mass M of the system is defined to be

Downloaded from https://www.cambridge.org/core. UNIVERSIDAD AUTONOMA METROPOLITANA, on 16 Nov 2026 at 19:59:29, subject to the Cambridge Core terms of use, available at https://www.cambridge.org/core/terms. https://doi.org/10.1017/9781009290098.002

$$M^2 = (\tilde{p}_1 + \tilde{p}_2)^2$$
$$= \tilde{p}_1^2 + \tilde{p}_2^2 + 2\tilde{p}_1 \cdot \tilde{p}_2$$
$$= m_1^2 + m_2^2 + 2(E_1 E_2 - p_1 p_2 \cos\theta) \quad (1.11)$$

where θ is the angle between the 3-vectors $\mathbf{p}_1$ and $\mathbf{p}_2$. The effective mass is a powerful tool for studying the properties of short-lived particles.

1.4 Summary of particle properties

Each of the particles mentioned previously has a unique set of properties that distinguish the particle and describe how it is affected by the fundamental interactions. These properties include

1. charge,
2. mass,
3. spin,
4. magnetic moment,
5. lifetime, and
6. branching ratios.

In addition, a full description of a particle must include the values for a set of internal quantum numbers, such as baryon number and strangeness [4]. The values of the internal quantum numbers determine which particles may be produced together in various reactions and how unstable particles can decay.

If we choose as a time interval the mean lifetime of a particle in its rest frame, then the particle lifetime in the LAB frame is generally longer due to the time dilation effect. The mean distance traveled in the LAB from production to decay is

$$\lambda_D = (p/mc)c\tau \quad (1.12)$$

Note that this grows linearly with the particle's momentum.

Suppose that N_0 unstable particles with mean decay length λ_D have been created at $x = 0$. The number of particle decays occurring in some small interval dx around the distance x is proportional to the number of particles at x and to the fractional size of the interval. Thus,

$$dN(x) = -N(x)\, dx/\lambda_D$$

from which it follows that

$$N(x) = N_0 \exp(-x/\lambda_D) \quad (1.13)$$

Thus, the decay lengths of unstable particles have an exponential distribution with a slope that depends on λ_D and hence on the $c\tau$ value of the particle. This can be useful sometimes in determining the identity of a decay sample.

We summarize in Table 1.1 the properties of the particles most com-

Downloaded from https://www.cambridge.org/core. UNIVERSIDAD AUTONOMA METROPOLITANA, on 16 Nov 2026 at 19:59:29, subject to the Cambridge Core terms of use, available at https://www.cambridge.org/core/terms. https://doi.org/10.1017/9781009290098.002

Downloaded from https://www.cambridge.org/core. UNIVERSIDAD AUTONOMA METROPOLITANA, on 16 Nov 2026 at 19:59:29, subject to the Cambridge Core terms of use, available at https://www.cambridge.org/core/terms. https://doi.org/10.1017/9781009290098.002

Table 1.1. *Properties of quasistable particles*

		Mass (MeV/c^2)	Spin ($\hbar$)	Magnetic moment	$c\tau$ (cm)	Major decay modes	Branching ratio (%)
Gauge bosons							
γ	photon	0	1	0	stable	—	—
Leptons							
ν_e	e neutrino	~0	$\frac{1}{2}$	0	stable	—	—
ν_μ	μ neutrino	~0	$\frac{1}{2}$	0	stable	—	—
e^-	electron	0.5110	$\frac{1}{2}$	$1.001\mu_B$	stable	—	—
μ^-	muon	105.7	$\frac{1}{2}$	1.001 ($e\hbar/2m_\mu c$)	6.59×10^4	$e\bar{\nu}\nu$	100
Mesons							
π^0	pion	135.0	0	0	2.5×10^{-6}	2γ	98.8
$\pi^\pm$	pion	139.6	0	0	780.4	$\mu\nu$	100
$K^\pm$	kaon	493.7	0	0	370.9	$\mu\nu$	63.5
						$\pi^\pm\pi^0$	21.2
						$\pi^\pm\pi^+\pi^-$	5.6
K_S^0	K short	497.7	0	0	2.675	$\pi^+\pi^-$	68.6
						$2\pi^0$	31.4
K_L^0	K long	497.7	0	0	1554	$\pi e\nu$	38.7
						$\pi\mu\nu$	27.1
						$3\pi^0$	21.5
						$\pi^+\pi^-\pi^0$	12.4

Downloaded from https://www.cambridge.org/core. UNIVERSIDAD AUTONOMA METROPOLITANA, on 16 Nov 2026 at 19:59:29, subject to the Cambridge Core terms of use, available at https://www.cambridge.org/core/terms. https://doi.org/10.1017/9781009290098.002

Baryons							
p	proton	938.3	$\frac{1}{2}$	$2.793\mu_N$	stable	—	—
n	neutron	939.6	$\frac{1}{2}$	$-1.913\mu_N$	2.7×10^{13}	$pe^-\bar{\nu}$	100
Λ	lambda	1115.5	$\frac{1}{2}$	$-0.613\mu_N$	7.89	$p\pi^-$	64.2
						$n\pi^0$	35.8
Σ^+	sigma	1189.4	$\frac{1}{2}$	$2.379\mu_N$	2.40	$p\pi^0$	51.6
						$n\pi^+$	48.4
Σ^0	sigma	1192.5	$\frac{1}{2}$		1.7×10^{-9}	$\Lambda\gamma$	100
Σ^-	sigma	1197.3	$\frac{1}{2}$	$-1.10\mu_N$	4.44	$n\pi^-$	100
Ξ^0	cascade	1314.9	$\frac{1}{2}$	$-1.25\mu_N$	8.69	$\Lambda\pi^0$	100
Ξ^-	cascade	1321.3	$\frac{1}{2}$	$-0.69\mu_N$	4.92	$\Lambda\pi^-$	100
Ω^-	omega	1672.5	$\frac{3}{2}$		2.46	ΛK^-	68.6
						$\Xi^0\pi^-$	23.4
						$\Xi^-\pi^0$	8.0

Source: Particle Data Group, Rev. Mod. Phys. 56: S1, 1984; L. Pondrom, in G. Bunce (ed.), *High Energy Spin Physics—1982,* AIP Conf. Proc. No. 95, 1983, p. 45.

monly encountered in particle physics. Listed are most particles that are not known to decay or that decay via the weak interaction and have a $c\tau$ value greater than 1 cm. We will refer to this group as the quasistable particles. We have also included the neutral members of the pion and sigma families, which decay by electromagnetic processes and thus have a much shorter lifetime than the other listed particles. Table 1.1 does not include the antiparticles, which have identical values for the listed properties, except for the charge and magnetic moment, which are opposite.

The mass of the photon is believed to be identically zero. Although the neutrino masses are very small, there is no compelling theoretical reason why they should be exactly zero. The spins of all particles are found to be multiples of $\hbar/2$, where $\hbar$ is Planck's constant divided by 2π. All neutrinos discovered to date have been "left handed." This means that the neutrino's spin is directed in the opposite direction from its momentum. Antineutrinos are right handed. The photon is the only particle in Table 1.1 to have a spin of 1, while the Ω^- is the only particle with spin $\frac{3}{2}$.

Particles with nonzero spin and nonzero mass have a magnetic moment associated with them. The natural unit for measuring magnetic moments is [5]

$$\mu = e\hbar/2Mc \tag{1.14}$$

where M is the particle's mass. When M equals the electron mass, μ is known as the Bohr magneton. When M is the proton mass, μ is called the nuclear magneton. Table 1.1 shows that the electron magnetic moment is $\sim m_p/m_e$ times larger than the baryon moments.

Apart from the free neutron, the longest lived of the unstable particles is the muon, with a $c\tau = 6.59 \times 10^4$ cm or $\tau = 2.2\ \mu$s. Also listed are the major decay modes of the decaying particles and the corresponding fractions (branching ratios) for each mode.

1.5 Scattering

Most of our knowledge about the interactions between particles has come from the analysis of scattering experiments. Consider the scattering of a beam particle (b) off a target particle (t) in the laboratory (LAB) frame, as shown in Fig. 1.2a. In high energy scattering a particle or group of particles is frequently found to be produced with a momentum comparable to p_b and with a direction close to the beam direction. Such a particle is referred to as the forward or scattered particle (1). In contrast, a second particle or group of particles is frequently found with lower momentum and at a larger angle with respect to the beam direction. This particle is

Downloaded from https://www.cambridge.org/core. UNIVERSIDAD AUTONOMA METROPOLITANA, on 16 Nov 2026 at 19:59:29, subject to the Cambridge Core terms of use, available at https://www.cambridge.org/core/terms. https://doi.org/10.1017/9781009290098.002

referred to as the backward or recoil particle (2). Such reactions are believed to proceed through the exchange of other (virtual) particles as shown in Fig. 1.2b. Two-body scattering takes its simplest form when viewed in the center of momentum (CM) frame, as shown in Fig. 1.2c.

A useful Lorentz invariant quantity related to the total energy involved in an interaction is

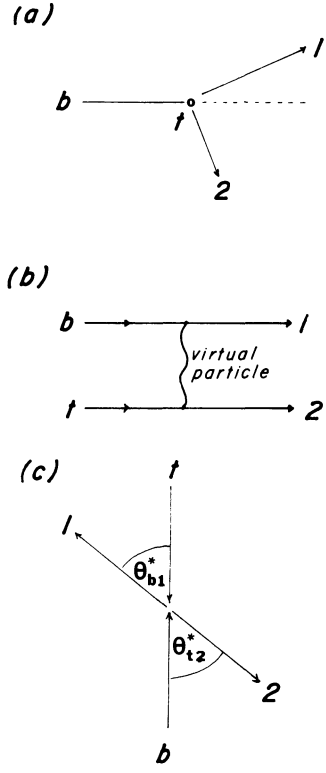
$$\begin{aligned} s &= (\tilde{p}_b + \tilde{p}_t)^2 \\ &= m_b^2 + m_t^2 + 2(E_b E_t - \mathbf{p}_b \cdot \mathbf{p}_t) \end{aligned} \tag{1.15}$$

If we evaluate these quantities in the CM coordinate system ($\mathbf{p}_b = -\mathbf{p}_t$), we find

$$\text{CM:} \qquad s = (E_b^* + E_t^*)^2 = W^2 \tag{1.16}$$

Quantities evaluated in the CM frame will be marked with an asterisk

Figure 1.2 (a) The $2 \rightarrow 2$ body scattering process in the LAB frame. The target particle is at rest. (b) The one-particle exchange diagram. (c) The $2 \rightarrow 2$ body scattering process in the CM system. The initial state particles have opposite momenta, as do the final state particles.



Downloaded from https://www.cambridge.org/core. UNIVERSIDAD AUTONOMA METROPOLITANA, on 16 Nov 2026 at 19:59:29, subject to the Cambridge Core terms of use, available at https://www.cambridge.org/core/terms. https://doi.org/10.1017/9781009290098.002

superscript. Thus, s gives the square of the total energy available in the CM system. Expressed in terms of LAB quantities ($p_t = 0$),

$$\text{LAB:} \qquad s = m_b^2 + m_t^2 + 2m_t E_b \tag{1.17}$$

At high energies, where we can neglect the mass terms, the total CM energy should grow like $(E_b)^{1/2}$.

A second Lorentz invariant quantity, which is related to the scattering angle, is the 4-momentum transfer from the beam to the forwardly scattered particle (or system)

$$\begin{aligned} t &= (\tilde{p}_b - \tilde{p}_1)^2 \\ &= m_b^2 + m_1^2 - 2(E_b E_1 - \mathbf{p}_b \cdot \mathbf{p}_1) \end{aligned} \tag{1.18}$$

The differential cross section $d\sigma/d\Omega$ depends on the frame in which the polar angle θ is measured. The cross section $d\sigma/dt$ on the other hand is Lorentz invariant since both σ and t are invariant. We can relate $d\sigma/dt$ to the CM angle by differentiating Eq. 1.18:

$$\frac{d\sigma}{dt} = \frac{d\sigma}{2\, p_b^* p_1^*\, d(\cos\theta^*)}$$

If there are no polarization effects, the differential cross section is independent of the azimuthal angle ϕ, and

$$\frac{d\sigma}{dt} = \frac{\pi}{p_b^* p_1^*} \frac{d\sigma}{d\Omega^*} \tag{1.19}$$

The relations between the kinematic variables of the particles are particularly simple in the CM system. If the incident energy and the masses of the particles are given and the dynamics of the scattering process is independent of azimuth, we have [6]

$$\begin{aligned} \theta_{t2}^* &= \pi - \theta_{b1}^* \\ p_b^* &= p_t^* = \frac{\Lambda^{1/2}(s, m_b^2, m_t^2)}{2(s)^{1/2}} \\ p_1^* &= p_2^* = \frac{\Lambda^{1/2}(s, m_1^2, m_2^2)}{2(s)^{1/2}} \end{aligned} \tag{1.20}$$

where the auxiliary function Λ is defined as

$$\Lambda(a, b, c) = a^2 + b^2 + c^2 - 2ab - 2ac - 2bc \tag{1.21}$$

The relations between the kinematic variables in the LAB frame are discussed in Appendix E.

It is possible to obtain a simple relation between the polar scattering angle θ^* in the CM frame and the polar angle θ in the LAB frame. We have

$$\tan\theta = p_T/p_z$$

Downloaded from https://www.cambridge.org/core. UNIVERSIDAD AUTONOMA METROPOLITANA, on 16 Nov 2026 at 19:59:29, subject to the Cambridge Core terms of use, available at https://www.cambridge.org/core/terms. https://doi.org/10.1017/9781009290098.002

where p_T (p_z) is the transverse (longitudinal) component of the particle's momentum. Suppose that the CM frame moves along z in the LAB. The velocity of the CM frame is

$$\beta_0 = \frac{p_0 c}{E_0} = \frac{p_b c}{(p_b^2 c^2 + m_b^2 c^4)^{1/2} + m_t c^2} \tag{1.22}$$

Now, p_T is invariant in the transformation from the CM to the LAB frame. However, the quantity p_z must obey the transformation law in Eq. 1.8. Thus, we have

$$\tan\theta = \frac{p_T^*}{\gamma_0(p_z^* + \beta_0 E^*/c)}$$

Dividing through by the magnitude of the particle's momentum p^*, we obtain

$$\tan\theta = \frac{\sin\theta^*}{\gamma_0(\cos\theta^* + \beta_0/\beta^*)} \tag{1.23}$$

Finally we derive an important result for the maximum energy that can be transferred from an incident particle to a target particle. Consider an incident particle with mass M and momentum p that has a headon collision with a target particle that has mass m and is initially at rest. In the CM frame the recoiling target particle has momentum and energy

$$p_r^* = mc\beta_0\gamma_0$$
$$E_r^* = mc^2\gamma_0$$

where β_0 is the velocity of the CM frame relative to the LAB frame. For cases with $M \gg m$

$$\beta_0 \simeq \frac{pc}{(p^2c^2 + M^2c^4)^{1/2}} = \beta$$

where β is the incident particle's velocity in the LAB. The energy of the recoil particle in the LAB can be determined from Eq. 1.8 by making a Lorentz transformation back to the LAB.

$$E_r \simeq \gamma c\left(\frac{E_r^*}{c} + \beta p_r^*\right)$$

Before the scattering occurred, this particle had only its rest energy mc^2. Thus, after substituting for $p_r^*$and E_r^*, we find that the maximum energy transfer is

$$\Delta E_{max} \simeq 2mc^2\beta^2\gamma^2 \tag{1.24}$$

Note that since the energy transfer is proportional to γ^2, the recoiling particle can receive a substantial amount of energy from an energetic

Downloaded from https://www.cambridge.org/core. UNIVERSIDAD AUTONOMA METROPOLITANA, on 16 Nov 2026 at 19:59:29, subject to the Cambridge Core terms of use, available at https://www.cambridge.org/core/terms. https://doi.org/10.1017/9781009290098.002

particle. The exact expression is [4]

$$\Delta E_{\max} = 2mc^2\beta^2\gamma^2 \left(1 + 2\gamma \frac{m}{M} + \frac{m^2}{M^2}\right)^{-1} \tag{1.25}$$

1.6 Particle physics experiments

It is an unfortunate fact of life that nature only begrudgingly reveals the secrets of her elementary particles. Huge experiments involving hundreds of people, years of effort, and the expenditure of millions of dollars may be necessary to measure the properties of new particles or the characteristics of particle interactions. Sometimes the elapsed time from an experiment's conception through its organization, construction, running at the accelerator, and data analysis to the publication of the results is so long that the original goals of the experiment are less important than other topics subsequently developed. In this and the following section we will attempt to give a cursory overview of a particle physics experiment. The subsequent chapters in the book will then treat each of the major topics in more detail.

Most detectors make use of the electromagnetic interactions of particles in matter (Chapter 2). For charged particles heavier than the electron, these interactions tend to be nondestructive because, apart from a small energy loss and a small momentum transfer, the particle is otherwise undisturbed. For these particles ionization of atomic electrons in the detector medium is the dominant source of energy loss. For high energy electrons the energy loss is mainly due to the production of photons through the bremsstrahlung process, while for high energy photons the main source of energy loss is through pair production. Thus, the interactions of high energy electrons and photons are destructive, since the initial particle is destroyed and replaced by a shower of lower energy particles.

The momentum transfer to charged particles is due to the Coulomb interaction of the particle with the nuclei in the medium. This momentum transfer causes small angular changes in the particle's trajectory. The nuclear interaction is important for neutral particles other than the photon and for high energy or large angle processes (Chapter 3).

Most experiments use a beam of particles produced and accelerated to high energy at a particle accelerator (Chapter 4). The main exceptions are experiments searching for evidence of nucleon decay, which look for a signal from a large volume of matter, free quark searches, and cosmic ray experiments. The beam from an accelerator is either directed into a fixed target or collided with a second counterrotating beam of particles. The

Downloaded from https://www.cambridge.org/core. UNIVERSIDAD AUTONOMA METROPOLITANA, on 16 Nov 2026 at 19:59:29, subject to the Cambridge Core terms of use, available at https://www.cambridge.org/core/terms. https://doi.org/10.1017/9781009290098.002

target for fixed target experiments is usually a small piece of metal or liquid hydrogen (Chapter 5). Spin-polarized targets and gas jets may also be used for special applications.

In a particle physics experiment detectors of various kinds are placed downstream of the fixed target or surrounding the collision point of colliding beams. Particles created in the collisions have electromagnetic or nuclear interactions in the detectors they pass through. The interaction usually creates an analog signal of some kind, which must be measured or converted into standardized pulses using fast pulse electronics (Chapter 6).

Detectors and other electronic apparatus are required for various purposes in every experiment. The tasks required for most experiments include

1. tracking,
2. momentum analysis,
3. neutral particle detection,
4. particle identification,
5. triggering, and
6. data acquisition.

Each detector has particular features for which it excels [7, 8]. The requirements for any given task are generally detrimental to others, so that experimental design requires careful optimization.

The spatial locations of the detector interactions may be combined by computer software to determine the trajectories of the particles. This is referred to as tracking. The most important characteristic of a tracking chamber is the spatial resolution, which measures the accuracy to which the position of the particle trajectory may be localized. Other important characteristics are the response time and the deadtime of the detector. The response time represents the time required to produce a signal after the passage of a particle. It includes the intrinsic time for the interaction between the particle and the detector medium and the time required to collect the photons or charges that were produced by the interaction. A second particle entering the detector during the response time will have its response mixed with the first. In some cases this presents a limitation on the maximum input event rate [7]. The recovery or deadtime is the length of time that must elapse following the passage of a particle before the detector can return to the condition it was in before the arrival of the particle. This time limits the rate at which the experiment can trigger the device. The event rate and average particle multiplicity influence the spatial and temporal resolution required in tracking detectors.

Downloaded from https://www.cambridge.org/core. UNIVERSIDAD AUTONOMA METROPOLITANA, on 16 Nov 2026 at 19:59:29, subject to the Cambridge Core terms of use, available at https://www.cambridge.org/core/terms. https://doi.org/10.1017/9781009290098.002

The excited atoms in certain materials can deexcite by emitting light. This is the basis of the scintillation counter (Chapter 7). The light must be efficiently collected and directed onto a photomultiplier tube. This tube first converts the light into an electrical signal and then amplifies the signal to a useful level. Scintillation counters are used for triggering and for particle identification using the time of flight technique.

Charged particles traveling in a dielectric medium with a velocity greater than the speed of light in the medium emit a form of radiation known as Cerenkov light (Chapter 8). This light can also be collected and converted using a photomultiplier tube. Cerenkov counters are used for particle identification.

Particles passing through a chamber containing a gas (or liquid argon) can decompose atoms into electrons and positive ions. If an electric field is present in the chamber, the two charged species drift apart. Near the positive electrode the electrons can acquire sufficient energy to create new ion pairs and a large electrical pulse can develop. This is the basis of the proportional chamber (Chapter 9). Large numbers of wires can be used in parallel to form a multiwire proportional chamber, which is useful for triggering and particle tracking.

In a drift chamber (Chapter 10), instead of detecting the collected charge from a chamber wire, one measures the time from some reference that the electrons take to drift to the wire. Drift chambers are most commonly used for tracking with good resolution. If the pulse height of the signal is also recorded, it is possible to use dE/dx for particle identification.

As mentioned, photons and electrons can create an electromagnetic shower. The characteristics of the shower can be measured with a sampling calorimeter (Chapter 11). A calorimeter usually consists of alternating layers of absorber and detectors. Showers initiated by high energy hadrons may likewise be measured with a hadron calorimeter.

There are a number of other detectors that are normally only used for special applications (Chapter 12). These include emulsions (excellent spatial resolution), bubble chambers and streamer chambers (large solid angle acceptance), transition radiation detectors (high energy particle identification), and silicon detectors (vertex information). Table 1.2 lists the most common uses for a number of detectors.

Every experiment needs a signal (trigger) to indicate when the spatial and temporal correlation of detector signals has determined that a potentially interesting event may have occurred (Chapter 13). The trigger may look for the characteristics of a certain type of particle or for a large

Downloaded from https://www.cambridge.org/core. UNIVERSIDAD AUTONOMA METROPOLITANA, on 16 Nov 2026 at 19:59:29, subject to the Cambridge Core terms of use, available at https://www.cambridge.org/core/terms. https://doi.org/10.1017/9781009290098.002

deposition of energy in a calorimeter. The system of detectors must efficiently signal the occurrence of the interesting events, even when they are accompanied by a large background of more common reactions. Microprocessors may be employed to make more complicated decisions based on a property of the particle or correlations between particles.

All the detectors in an experiment must be carefully integrated into a detector system (Chapter 14). If a set of tracking chambers is used in conjunction with a magnet, the resulting spectrometer may be used to measure the momentum of charged particles. System design involves a series of compromises on the size and location of the various detectors, the type and strength of magnetic field, the acceptance, segmentation, and rate handling capability. In large experiments careful attention must be given to calibration of the detector signals and to online monitoring of their performance.

Enormous amounts of analog and digital data are generated by the detectors in a large experiment. For example, Fig. 1.3 shows a display of drift chamber information from a high energy $\bar{p}p$ interaction. This data must be channeled via data acquisition systems into an online computer and then some storage medium such as magnetic tape for later data analysis. The data recording rate must be carefully matched with the trigger rate.

Sometimes it is necessary to know the identity (i.e., the mass) of at least some of the particles resulting from an interaction. Two separate kinematic measurements are necessary for particle identification. Usually one is provided by the momentum measurement. The second measurement

Table 1.2. *Detector uses*

Detector	Common uses	Chapter
Scintillation counter	tracking, fast timing, triggering	7
Cerenkov counter	particle identification, triggering	8
Proportional chamber	tracking, triggering	9
Drift chamber	tracking, particle identification	10
Sampling calorimeters	neutral particle detection, triggering	11
Bubble chamber	vertex detector, tracking	12.1
Emulsion	high resolution vertex detection	12.2
Spark chamber	tracking	12.3
Streamer chamber	vertex detector, tracking	12.4
Transition radiation detector	high energy particle identification	12.5
Semiconductor detector	vertex detector	12.6
Flashtube hodoscope	tracking	12.6
Spark counter	high resolution timing	12.6

Downloaded from https://www.cambridge.org/core. UNIVERSIDAD AUTONOMA METROPOLITANA, on 16 Nov 2026 at 19:59:29, subject to the Cambridge Core terms of use, available at https://www.cambridge.org/core/terms. https://doi.org/10.1017/9781009290098.002

then requires a specialized detector whose response is proportional to the velocity or energy of the particle.

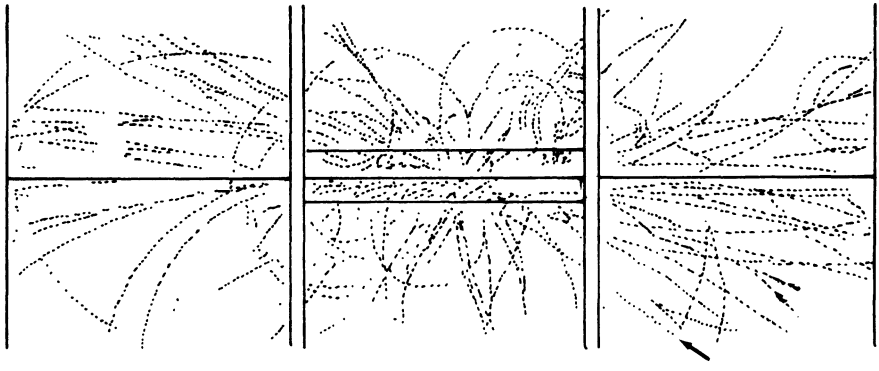
Finally, after one has selected an appropriate beam of particles and a target, an arrangement of magnetic field and detectors, a trigger, and a data acquisition system, one can do an experiment. Certain types of experiments are fundamentally important, such as those that measure the properties of particles or the total or elastic scattering cross sections (Chapter 15).

1.7 Data analysis

Computers play an essential role in particle physics experiments. We have already mentioned the use of online computers, which monitor the experiment and control the acquisition of data from the detectors. A second major use of computers is to process the data tapes through a series of programs that eventually yield the physics results the experiment was designed to obtain. This function is performed offline in the sense that the processing occurs independently of the experiment, although the same computers and much of the same software may be involved in both tasks. Much of this software is experiment, detector, or computer dependent. Therefore, we will only give a brief survey of the analysis tasks likely to be found in most experiments.

Table 1.3 outlines some common tasks for offline analysis. Of course, some experiments will not require all of these tasks, while others will need additional levels of processing. In general, as the processing level increases, software from different experiments tends to become more alike.

Figure 1.3 Particle trajectories in a $\bar{p}p$ collision with $W = 540$ GeV. The trajectories were determined from drift chamber hits. The electron track, indicated by the arrow, was identified using an electromagnetic calorimeter. This event was one of the first examples of a W vector boson decay. (After G. Arnison et al., Phys. Lett. 122B: 103, 1983.)



Downloaded from https://www.cambridge.org/core. UNIVERSIDAD AUTONOMA METROPOLITANA, on 16 Nov 2026 at 19:59:29, subject to the Cambridge Core terms of use, available at https://www.cambridge.org/core/terms. https://doi.org/10.1017/9781009290098.002

1.7.1 Preprocessing

The information from an experiment can appear in many different forms. It may, for example, include chamber wire numbers, drift times, photomultiplier tube signals, or scaler counts. All of this information must be written in some format on the permanent storage medium, which we take to be magnetic tape. The experimental signals may be channeled to the tape through a standard interface, such as CAMAC, or it may proceed through homemade electronics.

The information on the raw data tapes is usually organized into groups depending on the source of the information. Thus, for instance, beam chamber information may be in one group and drift chamber times in another. The data is usually packed as densely as possible in order to minimize the amount of tape required to record each event.

The first job for the preprocessor is to convert these stored records into a more manageable form. As a result, the preprocessor is the most experiment and computer dependent set of software. Data formatting routines unpack the experimental information and fill appropriate arrays that serve as input for the subsequent processing.

One of the most important software jobs is tracking. Thus, a second task of the preprocessing program is to calculate the spatial coordinates of all hits in the tracking chambers. The program applies predetermined calibration constants in order to convert the output of the devices into spatial coordinates. For example, the space–time relation for a drift chamber can be measured by scanning the position of the beam across a drift chamber cell and measuring the drift times. It is also necessary to determine the absolute positions of the chambers in some coordinate system. In order to do this, special alignment runs are performed with tracks whose trajectories have been determined independently. The alignment constants are adjusted until the deviations of the positions given by the chambers from the actual positions (residuals) are mini-

Table 1.3. *Offline analysis chain*

Level	Task	Purpose
1	Preprocessing	decodes raw data tapes, finds spatial coordinates
2	Pattern recognition	finds tracks, rough momentum with approximate field
3	Geometrical fitting	best track parameters using true field
4	Vertexing	associates tracks, particle decays
5	Kinematic fitting	assigns masses, finds missing neutrals
6	Physics analysis	finds effective masses, Dalitz plots, etc.

Downloaded from https://www.cambridge.org/core. UNIVERSIDAD AUTONOMA METROPOLITANA, on 16 Nov 2026 at 19:59:29, subject to the Cambridge Core terms of use, available at https://www.cambridge.org/core/terms. https://doi.org/10.1017/9781009290098.002

mized. In some chambers it may also be necessary to perform $\mathscr{E} \times B$ corrections on the apparent coordinates because of the motion of the electrical discharge in the fields.

It may also be possible to filter out certain classes of events at the preprocessing stage if it is known with certainty that they will fail a subsequent level of processing. For example, unless there are a minimum number of hits, pattern recognition will be unable to determine if a track was present. Eliminating such events as soon as possible minimizes the total processing time.

1.7.2 Pattern recognition

In order to do tracking, the programs must first recognize from the arrays of chamber hit positions when it is likely that the pattern of hits was caused by the passage of charged tracks and to determine the best values for the parameters describing the tracks. The first task is referred to as pattern recognition, while the second is known as geometrical fitting or more simply as geometry.

The pattern recognition program must take the arrays of spatial positions and determine when a set of hits represents a track. For 3-dimensional track reconstruction, information must be available for more than one plane. Typically a third set of planes may be used to resolve ambiguities. Pattern recognition is one of the most difficult software tasks. These programs must be carefully optimized for the specific experiment, the quality of the beam, and the performance of the tracking chambers. A large number of problems can arise, and specific algorithms must be available for every eventuality.

Several general methods of pattern recognition have been used for finding tracks [9]. A brute force examination of all possible combinations of hits is too time consuming for anything but the most simple experiments. Track following is a method commonly used with sets of closely spaced chambers. Here one starts with sets of three or four hits as far from the target or interaction region as possible so that the confusion of nearby tracks is minimized. The program then predicts the next few hits by extrapolating the assumed trajectory. If a chamber hit is present within a window determined by the errors on the extrapolation, the process is continued. On the other hand, if after taking into account the chamber efficiencies no more hits are found, the track may be abandoned. A vectorlike variation of this technique can be used when the chambers consist of closely spaced planes that measure more than one dimension of the trajectory. Then each chamber module gives a vector on the track, and one can search neighboring modules for corresponding vectors.

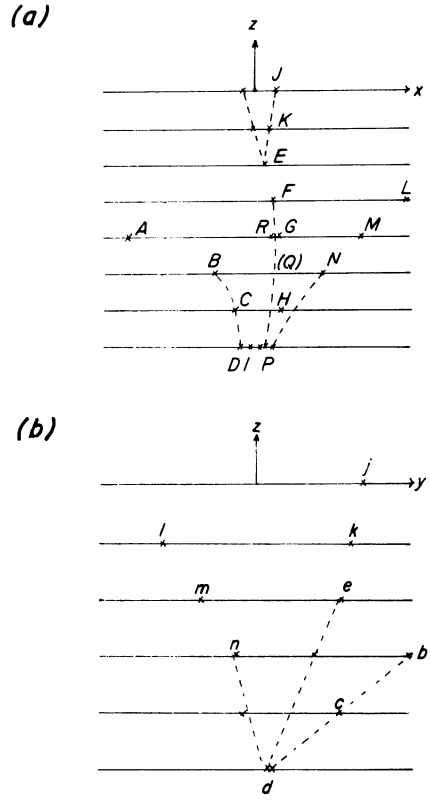
Downloaded from https://www.cambridge.org/core. UNIVERSIDAD AUTONOMA METROPOLITANA, on 16 Nov 2026 at 19:59:29, subject to the Cambridge Core terms of use, available at https://www.cambridge.org/core/terms. https://doi.org/10.1017/9781009290098.002

Another technique forms a track "road" by picking initial points near the beginning and end regions of chambers. If the track is curved, a third point near the center is also required. The program then uses a simple model of the trajectory and the measured position errors to define the road through the chambers and checks to see if additional hits lie on the road.

In some cases it is possible to use a global method of pattern recognition. If all the points on a given track have approximately the same value for some function of the coordinates, the tracks can be recognized by making a histogram of the function. The points belonging to a given track will cluster together. For example, the quantity y/x is the same for all points on a track in a field free region.

Some of the problems encountered in pattern recognition are illustrated in Fig. 1.4, which shows the pattern of hits in a set of chambers. Figure 1.4a shows the pattern measured perpendicular to the direction of

Figure 1.4 Pattern of chamber hits in two views.



Downloaded from https://www.cambridge.org/core. UNIVERSIDAD AUTONOMA METROPOLITANA, on 16 Nov 2026 at 19:59:29, subject to the Cambridge Core terms of use, available at https://www.cambridge.org/core/terms. https://doi.org/10.1017/9781009290098.002

the magnetic field (y), while Fig. 1.4b shows measurements in the plane containing the field. Assuming the field is approximately uniform, trajectories in the view perpendicular to the field form circular arcs. Now there must be some minimum requirements for what constitutes a track. Chambers may have spurious noise hits (A), while the chambers closest to the target may have many closely spaced hits (D, I, P). The position of each hit is only known to the accuracy of the chamber resolution. This makes it difficult to determine whether possible short track combinations such as BCD are really tracks. Examination of the hit patterns in the y-measuring planes may give additional confidence. In this view tracks lie along approximately straight lines. However, unless one is using specially constructed, 3-dimensional tracking chambers, the measurements in x and y occur at different values of z, and there is not an exact one-to-one correspondence between measurements in the two views. Since points b and c in Fig. 1.4b point back to the target, it is likely that BCD is a track, and that it appears so short because it is produced at a large angle with respect to the measuring planes.

The opposite problem from chamber noise is chamber inefficiency. Some tracks may have a missing hit (Q). Sometimes a track has a large angle multiple scattering or interaction in the chamber (E). This causes the apparent trajectory to appear as two broken segments. Another problem that can occur near the edge of a large magnet is nonuniformity in the field. This can cause a trajectory (LMN) to deviate smoothly from a circle in the xz view and from a line in the yz view.

1.7.3 *Geometrical fitting*

After the pattern recognition programs have determined which sets of chamber hits belong to tracks, it is necessary to obtain accurate measurements of the track parameters. Particle trajectories in a magnetic field $\mathbf{B}$ must satisfy the equation of motion

$$\frac{d^2\mathbf{x}}{ds^2} = \frac{q}{pc}\frac{d\mathbf{x}}{ds} \times \mathbf{B} \tag{1.26}$$

where q is the particle's charge, p is its momentum, and s is the distance along the trajectory. Neglecting energy loss, the solution of Eq. 1.26 is a straight line for a field free region and a helix for a uniform magnetic field. For these cases five parameters must be specified to define the trajectory: the coordinates x_0 and y_0 at some reference plane $z = z_0$, the magnitude of the momentum, and two angles to specify the direction.

Figure 1.5 shows the parameters for a helical trajectory in a uniform

Downloaded from https://www.cambridge.org/core. UNIVERSIDAD AUTONOMA METROPOLITANA, on 16 Nov 2026 at 19:59:29, subject to the Cambridge Core terms of use, available at https://www.cambridge.org/core/terms. https://doi.org/10.1017/9781009290098.002

magnetic field $\mathbf{B} = B\hat{e}_y$. The axis of the helix is parallel to the direction of the field. The dip angle λ measures the orientation of the momentum above or below the xz plane. The angle ϕ_0 is the azimuthal angle in the xz plane of the projection of the starting point with respect to the x axis. The projection of the trajectory onto the xz plane is a circle with radius of curvature given by

$$\rho = \frac{p \cos \lambda}{qB} \tag{1.27}$$

The projected curvature

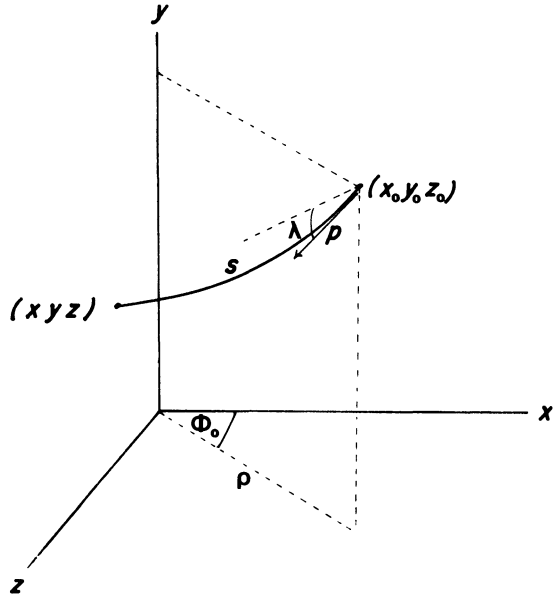
$$k = 1/\rho \tag{1.28}$$

is usually used as a track parameter instead of p because the error in k is constant for constant position measurement errors [9, 10]. Any point on the helix can be expressed as a function of the arc length traversed from the reference point as

$$\begin{aligned} x(s) &= (1/k)[\cos(\phi_0 + ks \cos \lambda) - \cos \phi_0] + x_0 \\ y(s) &= s \sin \lambda + y_0 \\ z(s) &= (1/k)[\sin(\phi_0 + ks \cos \lambda) - \sin \phi_0] + z_0 \end{aligned} \tag{1.29}$$

If the energy loss is appreciable, as it is for bubble chambers, the curvature is a function of s.

Figure 1.5 Definition of helical track parameters.



Downloaded from https://www.cambridge.org/core. UNIVERSIDAD AUTONOMA METROPOLITANA, on 16 Nov 2026 at 19:59:29, subject to the Cambridge Core terms of use, available at https://www.cambridge.org/core/terms. https://doi.org/10.1017/9781009290098.002

The curvature also varies if the magnetic field is nonuniform, in which case the trajectory may have to be broken up into segments. The trajectory through each segment is then either represented by a low order polynomial (spline fit) or determined by numerically integrating the equations of motion [9]. This is usually done by rewriting the x and y components of Eq. 1.26 in the form

$$\begin{aligned} x'' &= \frac{q}{pc}\frac{ds}{dz}[x'y'B_x - (1+x'^2)B_y + y'B_z] \\ y'' &= \frac{q}{pc}\frac{ds}{dz}[(1+y'^2)B_x - x'y'B_y - x'B_z] \end{aligned} \tag{1.30}$$

where the primes refer to derivatives with respect to z and

$$ds/dz = (1 + x'^2 + y'^2)^{1/2}$$

If the positions (x_n, y_n) and directions (x'_n, y'_n) of the trajectory are known at z_n, we can estimate their values at a nearby position z_{n+1} using Eq. 1.30 to give the second derivatives [11]. If we define $h_n = z_{n+1} - z_n$ and expand in a Taylor's series around z_n, we find

$$\begin{aligned} x_{n+1} &= x_n + x'_n h_n + 1/2 x''_n h_n^2 \\ x'_{n+1} &= x'_n + h_n x''_n \end{aligned} \tag{1.31}$$

with similar equations for y_{n+1} and y'_{n+1}. Then by reevaluating the second derivatives at z_{n+1}, one can continue stepping through the inhomogeneous magnetic field.

Once some model of the track trajectory has been adopted, the track parameters are determined by making a least squares fit to the measured spatial coordinates. Suppose we have a set of N chambers at fixed values of z. Then a χ^2 function can be defined by

$$\chi^2 = \sum_{i=1}^{N} \left[\frac{x_i - f(\omega; z_i)}{\sigma_i}\right]^2 \tag{1.32}$$

where x_i is the measured coordinate for the plane at z_i, σ_i is the error on the measurement, and $f(\omega; z_i)$ is the projection of the trajectory determined by the parameters ω onto the measurement plane. For a helical trajectory ω is the set $\{x_0, y_0, \phi_0, \lambda, k\}$. The parameter values are adjusted until the χ^2 function is minimized and

$$\frac{\partial \chi^2}{\partial \omega_j} = 0 \tag{1.33}$$

for each parameter ω_j. The least squares fitting procedure also produces a complete covariance matrix for the parameter errors.

Downloaded from https://www.cambridge.org/core. UNIVERSIDAD AUTONOMA METROPOLITANA, on 16 Nov 2026 at 19:59:29, subject to the Cambridge Core terms of use, available at https://www.cambridge.org/core/terms. https://doi.org/10.1017/9781009290098.002

1.7.4 Vertexing

The vertexing programs attempt to ascertain if isolated tracks originated from a common point. Bubble chamber analysis programs generally combine this task with kinematic fitting. All the tracks in a true event should originate from a production vertex or result from the decay of another particle that did.

In experiments using chambers for tracking, the geometrical tracks usually have to be extrapolated from the first chambers back toward the interaction region. This may require taking a series of small steps or making an initial pass with large tolerances if the magnetic field is inhomogeneous. The program then computes the distance of closest approach of the tracks, and tests if it is smaller than some minimum distance. Once two or more tracks are found that appear to be associated, the position of the actual vertex can be estimated by minimizing a χ^2 function defined in terms of the distances of the tracks to the assumed vertex point and the errors on the extrapolated tracks due to the errors on the track parameters. Alternatively, one could do an overall fit of the associated tracks to their chamber hits with the constraint that all the tracks must originate from a point.

In multivertex events the downstream decay vertices are found first. For vees the sum of the measured track momenta gives the momentum of the decaying particle. It can then be checked if the decaying particle is associated with the beam and other tracks at a production vertex. The tolerance that must be allowed for associating tracks is sensitive to the quality of the track measurements. Within the errors tracks may appear to come from more than one vertex. Thus, the physics questions under study may influence how the tracks are assigned to vertices.

1.7.5 Kinematic fitting

The complete kinematic description of an event requires that we specify the mass of each particle in addition to its momentum. For some tracks additional information may be available from particle identification detectors, such as Cerenkov counters or dE/dx chambers. The masses of the other tracks in an event are generally ambiguous. In this case one can assign various mass hypotheses to each of the tracks and perform a kinematic fit to the overall event. Given the mass assignments, the 4-vectors of the initial and final state systems are determined, and a true event must satisfy the laws of conservation of energy and momentum.

The fit proceeds by minimizing a χ^2 function defined in terms of the

Downloaded from https://www.cambridge.org/core. UNIVERSIDAD AUTONOMA METROPOLITANA, on 16 Nov 2026 at 19:59:29, subject to the Cambridge Core terms of use, available at https://www.cambridge.org/core/terms. https://doi.org/10.1017/9781009290098.002

difference between the track parameters and their geometry values as well as the errors on the track parameters [12]. Alternatively, one could consider the residuals of the tracks from the measured chamber hits. The energy–momentum constraints are added to the function using the method of Lagrangian multipliers. Since these constraints are nonlinear in the track parameters, the function must be minimized iteratively.

If all the tracks in an event have been well measured, there are four constraints ($4C$) on the overall fit. If there is a missing track, three constraints are lost in order to determine its momentum, and only one constraint ($1C$) remains on the fit. Multivertex events can be combined either by first fitting the downstream vertices and then working back toward the production vertex or by first fitting each vertex independently and then refitting them all simultaneously.

1.7.6 Physics analysis

It is obvious that this stage of the data analysis is totally experiment dependent. However, much of the software that is used at this stage is applicable to many different problems. Software should be available for making histograms and scatter plots of the data. When the 4-vectors of the particles are either fitted or assumed, effective masses, t distributions, Dalitz plots, and missing masses are commonly calculated. A number of cuts are usually applied to the data to obtain a clean sample of the particular types of events of interest.

Another important task at this stage is to understand the normalization for the data collected in the experiment. This is usually done by generating events using Monte Carlo (statistical) techniques and then propagating the created tracks through a simulation of the experimental apparatus. This allows one to find how the acceptance for various quantities in the experiment depend on known properties of the created tracks.

References

[1] D. Perkins, *Introduction to High Energy Physics,* 2nd ed., Reading: Addison-Wesley, 1982.
[2] G. t'Hooft, Gauge theories of the forces between elementary particles, Sci. Amer., June: 104–38, 1980. A fifth type of interaction has been proposed to explain the phenomenon of CP violation in K decays. At this point it is not clear if this is necessary.
[3] R. Hagedorn, *Relativistic Kinematics,* New York: Benjamin, 1964.
[4] Particle Data Group, Review of particle properties, Rev. Mod. Phys. 56: S1–S304, 1984.
[5] L. Pondrom, Magnetic moments of baryons and quarks, in G. Bunce (ed.), *High Energy Spin Physics—1982,* AIP Conference Proceeding No. 95, New York: AIP, 1983, pp. 45–57.

Downloaded from https://www.cambridge.org/core. UNIVERSIDAD AUTONOMA METROPOLITANA, on 16 Nov 2026 at 19:59:29, subject to the Cambridge Core terms of use, available at https://www.cambridge.org/core/terms. https://doi.org/10.1017/9781009290098.002

[6] W.S.C. Williams, *An Introduction to Elementary Particles,* 2nd ed., New York: Academic, 1971, pp. 491–4.
[7] C. Fabjan and H. Fischer, Particle detectors, Rep. Prog. Phys. 43: 1003–63, 1980.
[8] K. Kleinknecht, Particle detectors, Phys. Rep. 84: 85–161, 1982.
[9] H. Grote, Data analysis for electronic experiments, in C. Verkerk (ed.), Proc. of the 1980 CERN School of Computing, CERN Report 81-03, 1981, pp. 136–81.
[10] T. Fields, Magnets for bubble and spark chambers, in R. Shutt (ed.), *Bubble and Spark Chambers,* New York: Academic, 1967, pp. 1–50.
[11] J. Hart and D. Saxon, Track and vertex fitting in an inhomogeneous magnetic field, Nucl Instr. Meth. 220: 309–26, 1984.
[12] M. Alston, J. Franck, and L. Kerth, Conventional and semiautomatic data processing and interpretation, in R. Shutt (ed.), *Bubble and Spark Chambers,* New York: Academic, 1967, pp. 51–139.

Exercises

1. Suppose we express β for a particle in terms of the sine of some parametric angle θ, that is, $\beta = \sin\theta$. How are γ and p/m given in terms of θ?

2. What is the mean lifetime of a 100-GeV muon in the LAB frame?

3. For a 3-body final state with particles of masses m_1, m_2, and m_3, show that the lower limit for the effective mass of two of the particles is $m_1 + m_2$, and the upper limit is $W - m_3$, where W is the total energy in the CM frame.

4. Suppose in a hyperon production experiment we want a mean decay region of 1 m following the target. Find the required momentum for the produced hyperon for Λ, Σ^-, Ξ^-, Ω^-, and Σ^0.

5. What is the CM momentum of the π^- in the reaction $\pi^- p \rightarrow K^0\Lambda$ at a CM energy of 3 GeV? What is the CM momentum of the Λ? Can the K^0 be emitted in the backward hemisphere in the LAB?

6. What is the maximum energy transfer to an electron from a 100-GeV pion?

7. Suppose that the velocity of a certain particle in the CM frame β^* is less than the velocity β_0 of the CM in the LAB frame. Show that there is a maximum angle θ_{max} at which the particle may be emitted in the LAB given by

$$\tan\theta_{max} = \frac{\beta^*}{\gamma_0(\beta_0^2 - \beta^{*2})^{1/2}}$$

Downloaded from https://www.cambridge.org/core. UNIVERSIDAD AUTONOMA METROPOLITANA, on 16 Nov 2026 at 19:59:29, subject to the Cambridge Core terms of use, available at https://www.cambridge.org/core/terms. https://doi.org/10.1017/9781009290098.002

8. Make a rough flow chart for a pattern recognition program that takes into account the problems illustrated in Fig. 1.4.

9. Derive Eq. 1.26 starting from the Lorentz force equation. Derive Eq. 1.30.

10. Show that Eq. 1.29 is a solution to Eq. 1.26 for the case when $\mathbf{B} = B\hat{e}_y$.

Downloaded from https://www.cambridge.org/core. UNIVERSIDAD AUTONOMA METROPOLITANA, on 16 Nov 2026 at 19:59:29, subject to the Cambridge Core terms of use, available at https://www.cambridge.org/core/terms. https://doi.org/10.1017/9781009290098.002